Retinal Vessel Segmentation based on Hunger Games Search and Reptile Search Algorithms

MEHMET BAHADIR ÇETİNKAYA[1], HAKAN DURAN[2]
[1]Department of Mechatronics Engineering,
University of Erciyes,
38039, Melikgazi, Kayseri,
TURKEY

[2]Graduate School of Natural and Applied Sciences,
University of Erciyes,
38039, Melikgazi, Kayseri,
TURKEY

Abstract: - Metaheuristic algorithms may provide effective performance in image processing due to their strengthened random search abilities. In most of these algorithms, the intelligent collective behavior of animal swarms or individual intelligent behaviors of each animal is simulated. In this work, two recently proposed metaheuristic algorithms of hunger games search (HGS) and reptile search (RSA) algorithms are improved as clustering-based and then applied to the clustering of retinal image pixels. A detailed performance comparison is realized between HGS and RSA algorithms in terms of convergence speed, sensitivity, specificity, accuracy, mean squared error, standard deviation, and CPU time. Although HGS and RSA algorithms produce similar results in terms of clustering performance, it is observed that the HGS algorithm presents relatively better performance than the RSA algorithm in terms of all performance metrics. The simulation results obtained prove that HGS and RSA algorithms can successfully be used in retinal vessel segmentation.

Key-Words: - Retinal vessel segmentation, Clustering, DRIVE database, Metaheuristic algorithms, Hunger Games search algorithm, Reptile search algorithm.

Received: August 2, 2023. Revised: November 8, 2023. Accepted: December 19, 2023. Published: December 31, 2023.

1 Introduction

Segmentation of retinal vessels with high accuracy is vital in the diagnosis and treatment of retinal diseases. However, the analysis of retinal images is a complex process because of the close pixel values between the different regions of the image. To distinguish pixel values effectively, the clustering process has to be performed.

Before the segmentation process, firstly, the retinal images are subjected to pre-processings of band selection, bottom-hat transformation, and contrast enhancement. As a result of the band selection process, it is observed that the Green (G) layer of the Red-Green-Blue (RGB) image produces the best performance in terms of contrast and brightness. Afterward, the regions with worse contrast are enhanced by using a structural filter element in bottom-hat transformation. The expression of the bottom-hat transformation can be shown in Equation 1:

$$bottom-hat(g) = g - (g \bullet nB) \quad (1)$$

where g is the retinal image, B is the structural element that preferred as a disk with a radius of 8, and n is the bottom-hat transformation. Finally, the pixel values locally concentrated in narrow pixel intervals are distributed homogeneously to the whole pixel interval of [0 255] by applying a contrast enhancement process.

To present a more comprehensive analysis, the simulations were carried out on both healthy and diseased retinal images taken from the digital retinal images for vessel extraction (DRIVE) database and shown in Figure 1.

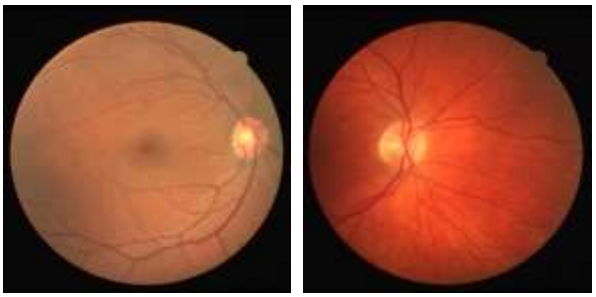

(a) Healthy (b) Diseased

Fig. 1: Retinal images taken from the DRIVE database

The retinal images obtained as a result of the three pre-processing operations are represented in Figure 2.

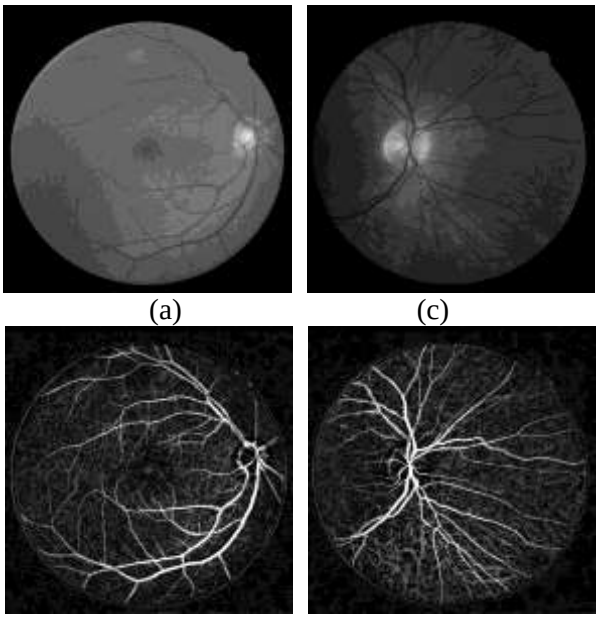

(a) (c)

(b) (d)

Fig. 2: (a) and (c) are the green layer images obtained as a result of band selection, (b) and (d) are the enhanced retinal images obtained after the bottom-hat transformation and contrast enhancement.

Metaheuristic algorithms perform the clustering operations directly on the retinal images given in Figure 2(b) and Figure 2(d).

2 Literature Review

To overcome the difficulties encountered in retinal vessel segmentation, metaheuristic algorithms can successfully be used. In literature, there are several works including the application of metaheuristic algorithms to retinal vessel segmentation. In [1], the authors proposed a glowworm swarm optimization (GSO) algorithm that automated detection of optic cups from retinal fundus images. An ant colony optimization (ACO) based approach is improved in [2], for optic cup segmentation in retinal fundus images. In work [3], the authors introduced an adaptive ant colony optimization (adaptive ACO) approach for edge detection-based retinal vessel segmentation. An improved binary processing-based artificial bee colony (ABC) algorithm is proposed in [4], for the aim of retinal vessel segmentation. The authors presented an accurate methodology in [5], that combines the lateral inhibition (LI) and the differential evolution (DE) approaches for retinal vessel and optic disc segmentation. In [6], a three-step methodology including a novel chaotic weighted elephant herding optimization (CWEHO) approach is introduced for retinal vessel segmentation. A novel approach that uses neural architecture search to optimize a U-net architecture using a binary teaching learning-based (BTLBO) algorithm is proposed in [7], for retinal vessel segmentation. In another work, an intelligent coyote optimization algorithm combined with deep learning is presented with the aim of detection and grading on retinal fundus images, [8]. In work [9], a hybrid approach consisting of an ant colony optimization algorithm and a machine learning technique is improved to classify the retinal pixels into regions containing blood vessels and not containing blood vessels. A novel neural architecture search approach for U-shaped networks is proposed in [10], with the aim of improving deep neural networks having high segmentation performance and lower inference time. In [11], the authors improved a novel differential evolution algorithm-based cross-entropy minimization procedure to perform an accurate pixel classification in retinal images. A new bio-inspired blood vessel segmentation hybrid technique using a bird swarm algorithm (BSA) and river formation dynamics (RFD) algorithm is presented in [12]. In work [13], an unsupervised retinal blood vessel segmentation approach based on the elite-guided multi-objective artificial bee colony (EMOABC) algorithm is proposed. The authors in [14], proposed a novel methodology for retinal vessel segmentation that is based on a bat algorithm and random forest classifier. In work [15], the authors presented a detailed and comparative research work including the application of the most effective heuristic algorithms to retinal vessel segmentation. Finally, in [16], a novel vessel segmentation approach using the multi-threshold-based remora optimization (MTRO) algorithm is presented.

3 Material and Methods

Hunger games search and reptile search algorithms are population-based metaheuristic approaches that simulate the intelligent behavior of animal herds or groups. In this work, HGS and RSA algorithms are improved as clustering-based and then applied to the retinal vessel segmentation.

HGS and RSA algorithms have the common control parameters of N and $MaxCycle$. In both algorithms, N represents the population size and $MaxCycle$ represents the maximum number of cycles.

3.1 Hunger Games Search Algorithm

HGS algorithm is a population-based metaheuristic algorithm inspired by the hunger driven activities and behavioral choices of animals. It was proposed in 2021, [17]. HGS algorithm can provide enhanced exploration and exploitation behaviors during the optimization process.

HGS algorithm includes five initialized parameters as N, $MaxCycle$, l and $SHungary$. Here, $SHungary$ can be defined as the total number of individuals feeling hungry while l and E are the control parameters that optimize the initial positions and search mode, respectively. $\overrightarrow{W_1}$ and $\overrightarrow{W_2}$ are the hunger weights that prevent the algorithm from getting stuck inside into a local minimum. Finally, $\vec{R}$ is a parameter used to optimize the variation rate of the search step, $\overrightarrow{X_b}$ represents the best solution of the current cycle, and BF is the best fitness of the current cycle.

The detailed pseudo-code of a basic HGS algorithm can be given as the following,

Initialize the parameters of $N, MaxCycle, l, SHungry$

Initialize individual positions, $X_i (i = 1, 2, ..., N)$

Cycle=1

While $Cycle < MaxCycle$

Calculate the fitness value of all individuals and determine the best solution producing the minimum *Euclidean distance*.

Update BF, WF, X_b

Calculate the $SHungry$ by,

$$hungry(i) = \begin{cases} 0, & AllFitness(i) = BF \\ hungry(i) + H, & AllFitness(i) \neq BF \end{cases}$$

where; $SHungry$ is the sum of hungry feelings of all individuals, namely, $hungry(i)$ and $AllFitness(i)$ represents the fitness of each individual in the current cycle.

Calculate the $\overrightarrow{W_1}$ by,

$$\overrightarrow{W_1(i)} = \begin{cases} hungry(i)\, x\, \dfrac{N}{SHungry}\, x\, r_4, & r_3 < 1 \\ 1, & r_3 > 1 \end{cases}$$

where; r_3 and r_4 are randomly produced numbers in the interval of [0,1].

Calculate the $\overrightarrow{W_2}$ by,

$$\overrightarrow{W_2(i)} = 1 - e^{-|hungry(i) - SHungry|}\ x\ r_5\, x 2$$

where; r_5 is a randomly produced number in the interval of [0,1].

For *Each Individual*

Calculate E by, $E = \sec h(|F(i) - BF|)$

where; $i \in (1, 2, ..., N)$, $F(i)$ represents the fitness value of each individual and $\sec h(x) = \dfrac{2}{e^x + e^{-x}}$ is a a hyperbolic function.

Update $\vec{R}$ by, $\vec{R} = 2\, x\, shrink\, x\, rand[0,1] - shrink$

where; $shrink$ can be determined as $2\, x\, (1 - \dfrac{Current\ Cycle}{MaxCycle})$ is a hyperbolic function.

Update all positions by,

$$\overrightarrow{X(t+1)} = \begin{cases} Game_1 : \overrightarrow{X(t)}\, x\, (1 + rand(1)), & r_1 < 1 \\ Game_2 : \vec{W_1}\, x\, \overrightarrow{X_b} + \vec{R}\, x\, \vec{W_2}\, x\, \left|\overrightarrow{X_b} - \overrightarrow{X(t)}\right|, & r_1 > l\,; r_2 > E \\ Game_3 : \vec{W_1}\, x\, \overrightarrow{X_b} - \vec{R}\, x\, \vec{W_2}\, x\, \left|\overrightarrow{X_b} - \overrightarrow{X(t)}\right|, & r_1 > l\,; r_2 < E \end{cases}$$

where; $rand(1)$ is a random number satisfying normal distribution and also r_1 and r_2 are randomly produced numbers in the interval of [0,1].

End For

Cycle= Cycle+1

End While

Return BF, X_b

UNTİL (termination criteria are met)

3.2 Reptile Search Algorithm

The RSA which was proposed in 2022 is a population based optimizer which simulates the hunting behavior of reptiles, especially crocodiles [18]. The encircling and the hunting phases of the RSA correspond to the exploration and exploitation

phases, respectively. The RSA can provide effective global search and local search abilities due to its robust exploration and exploitation behaviors.

β is a control parameter which optimizes the exploration accuracy for the encircling phase and α is a control parameter which optimizes the exploration accuracy for the hunting phase. Evolutionary Sense ($ES(t)$) represents a probability ratio taking randomly decreasing values between 2 and −2 throughout the cycles. In addition, $\eta_{(i,j)}$ parameter denotes the hunting operator for the j_{th} position in the i_{th} solution, $R_{(i,j)}$ is a value used to reduce the search space, and finally $P_{(i,j)}$ is the percentage difference between the j_{th} position of the optimal solution obtained so far and the j_{th} position of the current solution.

In RSA, to strengthen the encircling phase, the positions of the reptiles are updated via the following equation,

$$x_{(i,j)}(t+1) = \begin{cases} Best_j(t)\, x\, (-\eta_{(i,j)}(t))\ x\, \beta - R_{(i,j)}(t) \\ \quad x\ rand[0,1], \quad t \le \dfrac{MaxCycle}{4} \\ Best_j(t)\ x\ x_{(r,j)}\ x\ ES(t) \\ \quad x\ rand[0,1],\ t \le 2\dfrac{T}{4}\ and\ t > \dfrac{T}{4} \end{cases}$$

where; $Best_j(t)$ represents the j_{th} position of the optimal solution obtained so far and $x_{(r,j)}$ corresponds to a random position of the relevant solution ($x_{[(r1,r2,\ldots,rN),j]}$).

The detailed pseudo-code of a basic RSA algorithm can be given as the following,

Initialize the parameters of $N, MaxCycle, \alpha, \beta, \eta, R, P$
Randomly initialize the individual positions, $X: i = 1, 2, \ldots, N$
Cycle=1

While $Cycle < MaxCycle$
Calculate the fitness value for the candidate solutions and determine the best solution producing the minimum *Euclidean distance*.
Update ES by, $ES(t) = 2\,x\,r\,x\,(1 - \dfrac{1}{MaxCycle})$
where; r denotes to a random integer number between in [-1,1].

For $i = 1, 2, \ldots, N$
Update η, R, P parameters by,

$$\eta_{(i,j)} = Best_j(t)\, x\, P_{(i,j)}$$

$$R_{(i,j)} = \frac{Best_j(t)\ x\ x_{(r_2,j)}}{Best_j(t) + \varepsilon}$$

$$P_{(i,j)} = \alpha + \frac{x_{(i,j)} - M(x_i)}{Best_j(t)\, x\, (ub_j - lb_j) + \varepsilon}$$

where; ε a is a small value defined to prevent the denominator from being zero

If : *High Walking Phase*

$$Current\ Cycle \le \frac{MaxCycle}{4}$$

$$x_{(i,j)}(t+1) = Best_j(t)\, x\, (-\eta_{(i,j)}(t))\ x\ \beta - R_{(i,j)}(t)\, x\ rand[0,1]$$

Else : *Belly Walking Phase*

$$\frac{MaxCycle}{4} < Current\ Cycle \le 2\frac{MaxCycle}{4}$$

$$x_{(i,j)}(t+1) = Best_j(t)\ x\ x_{(r,j)}\ x\ ES(t)\ x\ rand[0,1]$$

Else : *Hunting Cooperation Phase*

$$2\frac{MaxCycle}{4} < Current\ Cycle \le 3\frac{MaxCycle}{4}$$

$$x_{(i,j)}(t+1) = Best_j(t)\, x\, (-\eta_{(i,j)}(t))\ x\ \beta - R_{(i,j)}(t)\, x\ rand[0,1]$$

End If

End For
Cycle= Cycle+1

End While
Return $Best(X)$: *best solution*
UNTİL (termination criteria are met)

For both HGS and RSA algorithms, the population size is chosen as 10 and the maximum cycle number is chosen as 100.

In the HGS algorithm, the value of the l parameter determines the rule to be chosen ($Game_1$, $Game_2$, …, $Game_X$) so the value of this parameter will be equal to the number of rules. The control parameter E controls the variation of all positions and its value can be calculated by using the formula given in pseudo code. Finally, the value of the

SHungry parameter is adaptively updated at each cycle depending on the hunger feelings of all individuals. In this work, the initial value of the *SHungry* parameter is set to zero.

In the RSA algorithm, the values of the β and α parameters are set to 0.1. The value of the η, R and P parameters are adaptively updated at each cycle depending on the equations given in the pseudo code. In this work, the initial value of the *SHungry* parameter is set to zero.

While measuring the success of the pixel clustering process, the Mean-Squared Error (MSE) criteria given in Equation 2 is used.

$$MSE = \frac{1}{N}\sum_{i=1}^{N}(f_i - y_i)^2 \quad (2)$$

where; N represents the total number of pixels, f_i is the value of the cluster center closest to the pixel i and y_i represents the pixel value of the i^{th} pixel.

4 Simulation Results

When the clustering based metaheuristic HGS and RSA algorithms improved for retinal vessel segmentation are applied to the retinal images given in Figure 1, the segmentation results obtained are shown in Figure 3. As seen from the results, HGS and RSA algorithms can distinguish the vessel and background pixels with high accuracy.

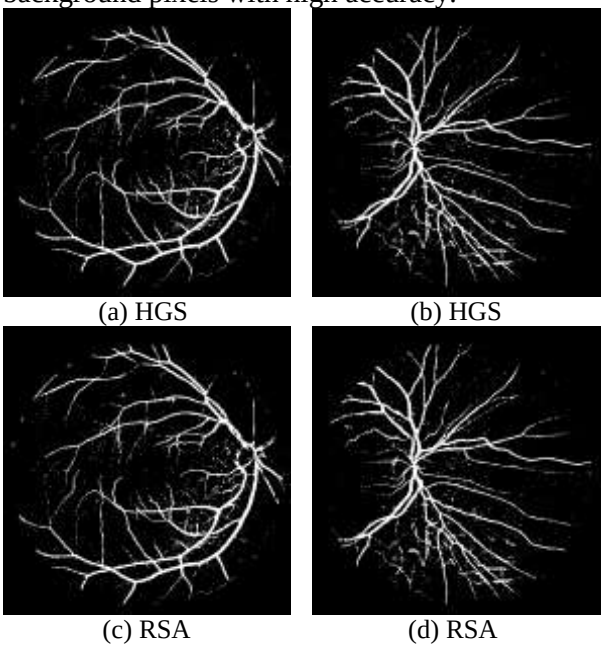

(a) HGS (b) HGS

(c) RSA (d) RSA

Fig. 3: Retinal images obtained after applying segmentation to the images given in Figure 1(a) and Figure 1(b) by using the clustering based HGS and RSA algorithms

In order to compare the convergence speeds of the algorithms, the mean convergence characteristics obtained for 20 random runs are shown in Figure 4. From the figure, it can be concluded that HGS can converge to the lower MSE values at fewer cycles.

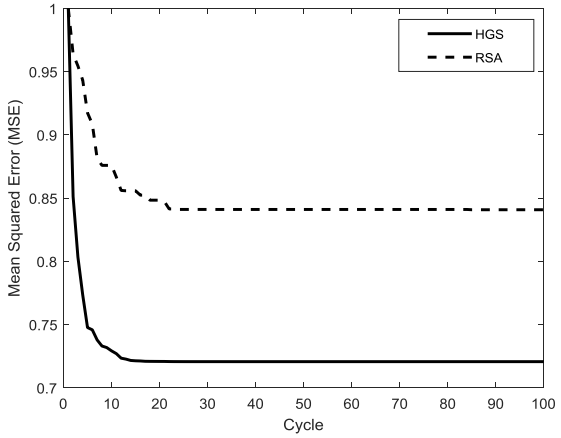

Fig. 4: Convergence speeds of the HGS and RSA algorithms

For a more detailed and fair comparison, the performances of the algorithms have also been evaluated in terms of sensitivity (*Se*), specificity (*Sp*), and accuracy (*Acc*) for all 20 retinal images in the DRIVE database. The mathematical expressions of *Se*, *Sp*, and *Acc* are represented in Equation 3-5 and the results obtained for each of the 20 retinal images are given separately in Table 1.

$$Se = \frac{TP}{(TP + FN)} \quad (3)$$

$$Sp = \frac{TN}{(TN + FP)} \quad (4)$$

$$Acc = \frac{TP + TN}{(TP + FN + TN + FP)} \quad (5)$$

In the equations given above, true positives (TP) represent the number of pixels that are vessels and have been detected as vessels. True negatives (TN) represent the correctly classified background pixels which can be considered non-vessel pixels. False positives (FP) represent the number of background pixels that are incorrectly classified as vessel pixels. False negatives (FN) represent the vessel pixels that have been incorrectly detected as background pixels. As a result, *Se* is the ratio of correctly classified vessel pixels while *Sp* is the ratio of

correctly classified background pixels and *Acc* is the ratio of correctly classified both the vessels and background pixels.

From the results obtained, it is observed that the performance of the HGS algorithm in terms of *Se*, *Sp*, and *Acc* is relatively better when compared to the RSA algorithm.

Table 1. The performance measures for the 20 different images taken from the DRIVE database

Image	Sensitivity		Specificity		Accuracy	
	HGS	RSA	HGS	RSA	HGS	HSA
1	0.8775	0.8869	0.9749	0.9793	0.9644	0.9625
2	0.8587	0.8502	0.9655	0.9698	0.9635	0.965
3	0.8616	0.873	0.9855	0.9807	0.9437	0.9294
4	0.8464	0.8378	0.9685	0.9648	0.9606	0.9626
5	0.8567	0.8487	0.9777	0.9665	0.9629	0.931
6	0.8458	0.8301	0.9718	0.9702	0.945	0.9271
7	0.8696	0.8282	0.9808	0.9622	0.9557	0.9406
8	0.8551	0.8623	0.9869	0.99	0.9225	0.8845
9	0.8847	0.8565	0.9973	0.9819	0.9367	0.9068
10	0.8589	0.8472	0.978	0.9855	0.9673	0.9457
11	0.8795	0.8474	0.9982	0.9716	0.9629	0.9633
12	0.8879	0.8398	0.9842	0.9879	0.9313	0.9405
13	0.8461	0.8461	0.9758	0.9599	0.9513	0.9513
14	0.8856	0.8379	0.9857	0.9714	0.9485	0.9408
15	0.8657	0.8257	0.9746	0.9746	0.9571	0.9571
16	0.8776	0.8599	0.9734	0.9813	0.9668	0.9552
17	0.8601	0.8695	0.9845	0.9818	0.9409	0.9178
18	0.8325	0.8625	0.971	0.971	0.9573	0.9573
19	0.861	0.8366	0.9759	0.9713	0.9593	0.9553
20	0.8952	0.8493	0.987	0.9821	0.9285	0.9372
Mean	0.86531	0.84978	0.97986	0.97519	0.95131	0.94155

The MSE values reached by the algorithms are also an important performance criterion. Simulation results represent that the HGS algorithm can converge to lower mean MSE values when compared to the RSA. Another performance metric to be analyzed is the standard deviation (σ) which represents the spread around the mean value. If the algorithm reaches close MSE values at each run, it can be defined as a statistically stable algorithm. From the results obtained, it is seen that HGS is more stable than RSA due to its lower standard deviation value. Finally, the CPU time which identifies the time interval required for a run, is another important performance metric. In this work, the simulations are realized on an Intel i7-10700 CPU with 2.0 GHz frequency and 16 GB RAM. In addition, the operating system is chosen as 64-bit Windows 10 Pro. When the minimum CPU time values obtained among 20 random runs for each algorithm are examined, it is seen that HGS produces better results than of RSA.

The results obtained for minimum MSE value, standard deviation, and CPU time are given in Table 2.

Table 2. Performance comparison of HGS and RSA algorithms in terms of minimum MSE values reached standard deviation, and CPU time

	Minimum MSE	Standard Deviation	CPU time (seconds)
HGS	0.7234	2.16438e-09	2.526588
RSA	0.8307	7.58405e-06	2.582861

To detect the statistically significant differences between the HGS and RSA algorithms, the Wilcoxon rank sum-test is also applied for the

confidence interval of 95% ($p<0.05$) and the results are given in Table 3.

Table 3. Wilcoxon sum-rank test results ($p<0.05$)

	Better than
HGS	RSA (6.7860e-08)
RSA	-

As seen from the Wilcoxon rank sum-test results, HGS produces more statistically significant results when compared to RSA.

5 Conclusion

In this work, HGS and RSA which are among the most novel metaheuristic algorithms are improved as clustering-based and then applied to retinal vessel segmentation. It has been observed that HGS and RSA algorithms can successfully distinguish the vessel pixels and background pixels which have close pixel values. The convergence analysis results show that the HGS algorithm requires 15 cycles to reach its optimal MSE value while the RSA requires 25 cycles. Furthermore, the HGS algorithm produces similar but a bit better results in terms of *Se*, *Sp*, and *Acc* metrics when compared to RSA. Similarly, the performance of the HGS algorithm in terms of the minimum MSE value reached and CPU time seems a bit better according to the RSA algorithm. Finally, the higher standard deviation value of HGS proves that it is statistically more stable than the RSA algorithm. In future works, the HGS and RSA algorithms will be improved as clustering-based for the analysis of different biomedical images and then their performances will be compared with other novel metaheuristic algorithms.

References:

[1] Pruthi, J., Khanna, K., Arora, S., Optic Cup segmentation from retinal fundus images using Glowworm Swarm Optimization for glaucoma detection, *Biomedical Signal Processing and Control*, Vol. 60, Article Id:102004, 2020, https://doi.org/10.1016/j.bspc.2020.102004.

[2] Arnay, R., Fumero, F., Sigut, J., Ant Colony Optimization-based method for optic cup segmentation in retinal images, *Applied Soft Computing*, Vol. 52, No. 2017, 2017, pp. 409-417, https://doi.org/10.1016/j.asoc.2016.10.026.

[3] Liantoni, F., Rozi, N.F., Indriyani, T., Rahmawati, W.M., Hapsari, R.K., Gradient based ant spread modification on ant colony optimization method for retinal blood vessel edge detection, *IOP Conference Series: Materials Science and Engineering, Vol. 1010, The 2nd International Conference on Advanced Engineering and Technology (ICATECH 2020)*, 2020, Indonesia.

[4] Pan, X., Zhang, Q., Pan, H., Improved artificial bee colony algorithm and its application to fundus retinal blood vessel image binarization, *IEEE Access*, Vol. 8, 2020, pp. 123726-123734, https://doi.org/10.1109/ACCESS.2020.3001299.

[5] Diaz, P., Rodriguez, A., Cuevas, E., Valdivia, A., Chavolla, E., Cisneros, M.P., Zaldivar, D., A hybrid method for blood vessel segmentation in images, *Biocybernetics and Biomedical Engineering*, Vol. 39, No. 3, 2019, pp. 814-824, https://doi.org/10.1016/j.bbe.2019.06.009.

[6] Kaur, A., Kaur, M., A novel chaotic weighted EHO-based methodology for retinal vessel segmentation, *Computer Methods in Biomechanics and Biomedical Engineering: Imaging & Visualization*, Vol. 11, No. 7, 2023, pp. 2894-2916, https://doi.org/10.1080/21681163.2023.2285455.

[7] Rajesh, C., Kumar, S., *Automatic retinal vessel segmentation using BTLBO.* In: Thakur, M., Agnihotri, S., Rajpurohit, B.S., Pant, M., Deep, K., Nagar, A.K. (eds) Soft Computing for Problem Solving, *Lecture Notes in Networks and Systems*, Vol. 547, Springer, 2023.

[8] Parthiban, K., Kamarasan, M., Diabetic retinopathy detection and grading of retinal fundus images using coyote optimization algorithm with deep learning, *Multimedia Tools and Applications*, Vol. 82, 2023, pp. 18947-18966, https://doi.org/10.1007/s11042-022-14234-8.

[9] Devarajan, D., Ramesh, S.M., Gomathy, B., A metaheuristic segmentation framework for detection of retinal disorders from fundus images using a hybrid ant colony optimization, *Soft Computing*, Vol. 24, No. 17, 2020, pp. 13347-13356, https://doi.org/10.1007/s00500-020-04753-7.

[10] Kuş, Z, Kiraz, B., Evolutionary architecture optimization for retinal vessel segmentation, IEEE *Journal of Biomedical and Health*

Informatics, Vol. 27, No. 12, 2023, pp. 5895-5903, https://doi.org/10.1109/JBHI.2023.3314981.

[11] Cuevas, E., Rodríguez, A., Alejo-Reyes, A., Del-Valle-Soto, C., *Blood vessel segmentation using differential evolution algorithm*, In: Studies in Computational Intelligence, Vol. 948, Springer, 2021.

[12] Pruthi, J., Arora, S., Khanna, K., *Segmentation of blood vessels from retinal fundus images using bird swarm algorithm and river formation dynamics algorithm.* In: Algorithms for Intelligent Systems, Springer, 2019.

[13] Bilal, K., Christodoulidis, A., Djerou, L., Babahenini, M.C., Cheriet,F., Retinal blood vessel segmentation using the elite-guided multi-objective artificial bee colony algorithm, *IET Image Processing*, Vol. 12, No. 12, 2018, pp. 2163-2171, https://doi.org/10.1049/iet-ipr.2018.5425.

[14] Sathananthavathi, V., Indumathi, G., BAT algorithm inspired retinal blood vessel segmentation, *IET Image Processing.* Vol.12, No.11, 2018, pp. 2075-2083, https://doi.org/10.1049/iet-ipr.2017.1266.

[15] Çetinkaya, M.B., Duran, H., A detailed and comparative work for retinal vessel segmentation based on the most effective heuristic approaches. *Biomedical Engineering-Biomedizinische Technik*, Vol. 66, No. 2, 2021, pp. 181–200, https://doi.org/10.1515/bmt-2020-0089.

[16] Vinayaki, V.D., Kalaiselvi, R., Multithreshold image segmentation technique using remora optimization algorithm for diabetic retinopathy detection from fundus images, *Neural Processing Letter*s, Vol. 54, No. 3, 2022, pp. 2363–2384, https://doi.org/10.1007/s11063-021-10734-0.

[17] Yang, Y., Chen, H., Heidari, A.A., Gandomi, A.H., Hunger Games Serach: Visions, conception, implementation, deep analysis, perspectives, and towards performance shifts, *Expert Systems with Applications*, Vol. 177, Article Id:114864, 2021, https://doi.org/10.1016/j.eswa.2021.114864.

[18] Abualigah, L., Elaziz, M. A., Sumari, P., Geem, Z. W., Reptile Search Algorithm (RSA): A nature-inspired meta-heuristic optimizer, *Expert Systems with Applications*, Vol. 191, Article Id:116158, 2022, https://doi.org/10.1016/j.eswa.2021.116158.

Contribution of Individual Authors to the Creation of a Scientific Article (Ghostwriting Policy)

The authors equally contributed to the present research, at all stages from the formulation of the problem to the final findings and solution.

Sources of Funding for Research Presented in a Scientific Article or Scientific Article Itself

No funding was received for conducting this study.

Conflict of Interest

The authors have no conflicts of interest to declare.